

## **A SIGNAL COVERAGE MODEL FOR TWO NEIGHBORING ISLANDS OF DIFFERENT SIZE**

**C. A. Valagiannopoulos**

School of Electrical and Computer Engineering  
National Technical University of Athens  
Heroon Polytechniou 9, GR-15773 Zografou, Athens, Greece

**Abstract**—Point source scattering by two rectangular dielectric obstacles on a perfectly conducting screen is studied by solving approximately the integral equations resulting from the scattering theorem. The configuration can be used as a model describing antenna radiation over the sea in the presence of two islands, one of which is much larger than the other. The approach is scalar and two-dimensional, while a linear system, produced via analytical integrations, is derived to evaluate the field inside the scatterers. The received power on the two islands is presented in several diagrams as function of the material and distance parameters to estimate the signal coverage across the two regions.

### **1. INTRODUCTION**

The correct operation of different equipment which use electromagnetic phenomena and the avoidance of interference effects from the surrounding area are commonly investigated using electromagnetic scattering techniques. Thus, electromagnetic compatibility naturally focuses on wave scattering by various structures. In [1], the FDTD method is implemented to develop a general technique in treating various field scattering problems. The derived near-field equivalent currents are used to determine the far-field features of the formations. Also in [2], a study concerning the electromagnetic scattering by obstacles above a lossy half space is presented. Through the moment solution, one can observe the shield effects and estimate the echo widths for several scatterers. Wait has additionally examined a laterally anisotropic surface excited by a vertical electric dipole [3]. The waves get trapped just above the surface when specific impedance condition

is in effect. Furthermore, an improved formulation for the electric-type integral equation has been developed to increase the efficiency of the solution to three-dimensional problems of electromagnetic scattering [4]. The method is suitable for conducting targets with sharp surfaces.

Propagation of electromagnetic waves over sea or ground is a classical problem that has attracted the interest of both theoretical researchers and experimental scientists. Except for its obvious practical significance in wireless terrestrial communications, this topic can be intriguing from the aspect of electromagnetic compatibility as the propagation features and the radiator characteristics are affected by the surrounding environment. In [5], Schlessinger studies the induced currents on an infinite wire above a penetrable earth under plane wave excitation. The phase coherence between the incident and the wire field is noted, while the dependence of the system propagation constants on the operating wavelength and the permittivity of the ground are highlighted. Furthermore, a thorough analysis of the cross polarization in radar return from a rough sea surface is given in [6]. The authors obtain explicit forms for the elements of the polarization matrix and discuss their variations with respect to the geometrical parameters. Finally, the radiation of a vertical dipole above a lossy spherical earth has been extensively developed in [7]. Analytical formulas for the ground wave amplitude are extracted and their behavior with varying the observing distance is investigated.

In this work, we examine point source scattering by two rectangular dielectric volumes on a perfectly conducting half space. This configuration can be considered as an overwater propagation model for two neighboring islands. A study with similar motivation is provided in [8]. The excitation is an infinite dipole and the shape of the geometry is two-dimensional; as a result, the scattering problem is reduced to a scalar one. The Green's function of the radiation area in the absence of the two dielectric formations is straightforwardly computed via image theory. We formulate an integral equation whose unknown functions are the fields inside the volumes of the two islands. The shape of the scatterers is not canonical (e.g., circle) and therefore their cross sections are discretized and a stepwise approximation is adopted for the unknown fields. The field values are computed by inverting a well-defined linear system whose matrix elements are analytically evaluated [9]. The scope of this work is to study the average field on the main island in the presence of the neighboring one and to examine the possibility to have field coverage of the neighboring island's area by an antenna located above the main one. Several diagrams of the related signal quantities with respect to the materials

and the magnitudes of the supersea volumes, the operating frequency, the height of the source, and the inter-island distance are shown and discussed.

**2. PROBLEM STATEMENT AND MATHEMATICAL FORMULATION**

Consider a perfectly conducting (PEC) planar half space on which are located two separate rectangular obstacles (regions 1 and 2) of lossy and magnetically inert materials. Their lengths are denoted by  $L_1$ ,  $L_2$  with  $L_1 > L_2$  and their heights by  $h_1$ ,  $h_2$  respectively. The symbols  $\epsilon_1$ ,  $\epsilon_2$  are used for the complex relative dielectric constants of the corresponding materials with conductivities  $\sigma_1$ ,  $\sigma_2$ . The distance between the two volumes equals  $D$ , while the background medium is vacuum (region 0) with wavenumber  $k_0$ . The wavenumbers inside regions 1 and 2 are referred to as  $k_1$  and  $k_2$  respectively. The investigated physical configuration is depicted in Fig. 1 where the cartesian coordinate system  $(x, y, z)$  used, is also defined. The PEC surface coincides with the  $x$ - $z$  plane and the  $y$  axis is positioned in the middle of the first formation. The structure is excited by an electric

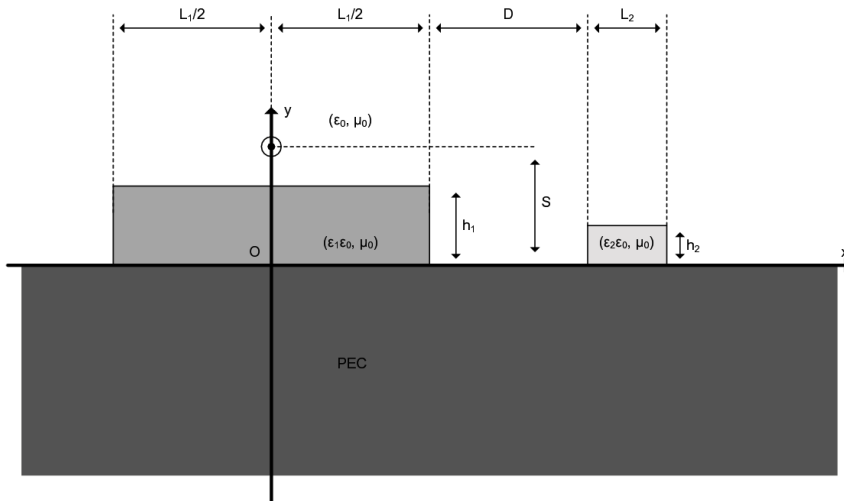


**Figure 1.** The geometry of the investigated model. Two rectangular volumes (representing islands) exist on a perfectly conducting half space (representing sea). The structure is excited by a two-dimensional dipole located above the first island.

dipole of constant current  $-I$  (opposite axial direction, expressed in  $A$ ), infinite towards the  $z$  axis, placed on  $y$  axis above the first rectangular volume at height  $S > h_1$ .

Both the shape and the excitation of the system are invariant across the  $z$  axis. Therefore, the only nonzero electric component is the axial one  $E_z = E$ , while the problem is reduced to a scalar and two-dimensional one. It should be stressed that the PEC half space represents the sea which possesses high conductivity. The two lossy rectangular volumes, supposed to be homogeneous, correspond to islands of different surface types and sizes. The antenna source is located above the first island which is the larger one. Each field quantity is written with a subscript indicating the region to which it is referred. Our analysis is harmonic and a time dependence of the form  $\exp(+j2\pi ft)$  is adopted and suppressed throughout, where  $f$  is the operating frequency.

The two islands are considered as scatterers placed on the surrounding environment of the PEC half space. Consequently, both the Green's function  $G$  and the incident axial electric field  $E_{0,inc}$  are computed in the absence of the rectangular dielectric volumes. The electric-type Green's function for such a two-dimensional configuration is defined as the axial electric field developed by an elementary dipole of magnitude  $j/(k_0\zeta_0)$  (expressed in  $A$ ) located along the axis ( $x = X, y = Y$ ) belonging in the upper (vacuum) half space. The notation  $\zeta_0$  is used for the free space intrinsic impedance. A closed form for the Green's function is available with use of the image theory [10, p. 90]:

$$G(x, y, X, Y) = -\frac{j}{4}H_0^{(2)}\left(k_0\sqrt{(x-X)^2 + (y-Y)^2}\right) + \frac{j}{4}H_0^{(2)}\left(k_0\sqrt{(x-X)^2 + (y+Y)^2}\right), \quad (1)$$

where  $H_u^{(2)}$  is the Hankel function of  $u$ -th order and second type. The observation point  $(x, y)$  lies also at the vacuum region 0. As far as the related incident electric field is concerned, a similar formula is obtained:

$$E_{0,inc}(x, y) = -\frac{k_0\zeta_0 I}{4}H_0^{(2)}\left(k_0\sqrt{x^2 + (y-S)^2}\right) + \frac{k_0\zeta_0 I}{4}H_0^{(2)}\left(k_0\sqrt{x^2 + (y+S)^2}\right). \quad (2)$$

By exploiting the reciprocity of the Green's function, the magnetic inertia of the participating materials and the second Green's integral formula [10, p.791], one can prove the validity of the scattering theorem, extensively used in previous works [11–17] which in our case

is particularized to give:

$$\begin{aligned}
 E(x, y) = & E_{0,inc}(x, y) + (k_1^2 - k_0^2) \int_0^{h_1} \int_{-L_1/2}^{L_1/2} G(x, y, X, Y) E(X, Y) dX dY \\
 & + (k_2^2 - k_0^2) \int_0^{h_2} \int_{L_1/2+D}^{L_1/2+D+L_2} G(x, y, X, Y) E(X, Y) dX dY \quad (3)
 \end{aligned}$$

where  $x \in R$  and  $y > 0$ , as the electric field is identically zero across the lower half space. It is apparent that the field of the entire area can be computed via the (unknown) values of the total field  $E(x, y)$  into the dielectric scatterers. Hence, formula (3) is applied for the internal points of these penetrable objects to yield a pair of integral equations for the unknown functions  $E_1(x, y)$  and  $E_2(x, y)$ . The first one stands for  $x \in [-L_1/2, L_1/2]$  and  $y \in [0, h_1]$  (first island, region 1) and is written as:

$$\begin{aligned}
 E_1(x, y) = & E_{0,inc}(x, y) + (k_1^2 - k_0^2) \int_0^{h_1} \int_{-L_1/2}^{L_1/2} G(x, y, X, Y) E_1(X, Y) dX dY \\
 & + (k_2^2 - k_0^2) \int_0^{h_2} \int_{L_1/2+D}^{L_1/2+D+L_2} G(x, y, X, Y) E_2(X, Y) dX dY. \quad (4a)
 \end{aligned}$$

The second one is valid for  $x \in [L_1/2 + D, L_1/2 + D + L_2]$  and  $y \in [0, h_2]$  (second island, region 2) and takes the form:

$$\begin{aligned}
 E_2(x, y) = & E_{0,inc}(x, y) + (k_1^2 - k_0^2) \int_0^{h_1} \int_{-L_1/2}^{L_1/2} G(x, y, X, Y) E_1(X, Y) dX dY \\
 & + (k_2^2 - k_0^2) \int_0^{h_2} \int_{L_1/2+D}^{L_1/2+D+L_2} G(x, y, X, Y) E_2(X, Y) dX dY. \quad (4b)
 \end{aligned}$$

### 3. APPROXIMATE SOLUTION OF THE INTEGRAL EQUATIONS

With a slight loss of generality, it is assumed that the islands dimensions are integer multiples of an electrically small distance  $a$ .

In particular, we suppose that:

$$L_1 = 2N_{x1}a \quad h_1 = N_{y1}a \quad (5a)$$

$$L_2 = N_{x2}a \quad h_2 = N_{y2}a \quad (5b)$$

where  $N_{x1}$ ,  $N_{y1}$ ,  $N_{x2}$  and  $N_{y2}$  are integer numbers. In order to manipulate the integral equations (4a) and (4b), the penetrable scatterers are divided into many identical square pixels of area  $a^2$  [9]. The electric field is assumed to not vary within the limits of a single square and to equal to its value at the center of the pixel. Therefore, the unknowns for the field in the first island are the quantities  $E_1(x_1(n_{x1}), y_1(n_{y1}))$  with  $n_{x1} = 1, \dots, 2N_{x1}$  and  $n_{y1} = 1, \dots, N_{y1}$ . The unknowns for the field in the second island are the quantities  $E_2(x_2(n_{x2}), y_2(n_{y2}))$  with  $n_{x2} = 1, \dots, N_{x2}$  and  $n_{y2} = 1, \dots, N_{y2}$ , where the coordinates of the centers for each small square are given by:

$$x_1(n_{x1}) = \left(n_{x1} - N_{x1} - \frac{1}{2}\right)a \quad y_1(n_{y1}) = \left(n_{y1} - \frac{1}{2}\right)a \quad (6a)$$

$$x_2(n_{x2}) = \frac{L_1}{2} + D + \left(n_{x2} - \frac{1}{2}\right)a \quad y_2(n_{y2}) = \left(n_{y2} - \frac{1}{2}\right)a. \quad (6b)$$

In this way, a  $(2N_{x1}N_{y1} + N_{x2}N_{y2}) \times (2N_{x1}N_{y1} + N_{x2}N_{y2})$  linear system is formed with respect to the discrete values of the total electric field across the volume of the scatterers. More specifically:

$$\begin{aligned} & (k_1^2 - k_0^2) \sum_{n_{y1}=1}^{N_{y1}} \sum_{n_{x1}=1}^{2N_{x1}} E_1(x_1(n_{x1}), y_1(n_{y1})) \int_{y_1(n_{y1}) - \frac{a}{2}}^{y_1(n_{y1}) + \frac{a}{2}} \int_{x_1(n_{x1}) - \frac{a}{2}}^{x_1(n_{x1}) + \frac{a}{2}} \\ & G(x_1(m_{x1}), y_1(m_{y1}), X, Y) dXdY + (k_2^2 - k_0^2) \sum_{n_{y2}=1}^{N_{y2}} \\ & \sum_{n_{x2}=1}^{N_{x2}} E_2(x_2(n_{x2}), y_2(n_{y2})) \int_{y_2(n_{y2}) - \frac{a}{2}}^{y_2(n_{y2}) + \frac{a}{2}} \int_{x_2(n_{x2}) - \frac{a}{2}}^{x_2(n_{x2}) + \frac{a}{2}} \\ & G(x_1(m_{x1}), y_1(m_{y1}), X, Y) dXdY - E_1(x_1(m_{x1}), y_1(m_{y1})) \\ & = -E_{0,inc}(x_1(m_{x1}), y_1(m_{y1})) \end{aligned} \quad (7a)$$

$$\begin{aligned}
 & (k_1^2 - k_0^2) \sum_{n_{y1}=1}^{N_{y1}} \sum_{n_{x1}=1}^{2N_{x1}} E_1(x_1(n_{x1}), y_1(n_{y1})) \int_{y_1(n_{y1})-\frac{a}{2}}^{y_1(n_{y1})+\frac{a}{2}} \int_{x_1(n_{x1})-\frac{a}{2}}^{x_1(n_{x1})+\frac{a}{2}} \\
 & G(x_2(m_{x2}), y_2(m_{y2}), X, Y) dXdY + (k_2^2 - k_0^2) \sum_{n_{y2}=1}^{N_{y2}} \sum_{n_{x2}=1}^{N_{x2}} \\
 & E_2(x_2(n_{x2}), y_2(n_{y2})) \int_{y_2(n_{y2})-\frac{a}{2}}^{y_2(n_{y2})+\frac{a}{2}} \int_{x_2(n_{x2})-\frac{a}{2}}^{x_2(n_{x2})+\frac{a}{2}} \\
 & G(x_2(m_{x2}), y_2(m_{y2}), X, Y) dXdY - E_2(x_2(m_{x2}), y_2(m_{y2})) \\
 & = -E_{0,inc}(x_2(m_{x2}), y_2(m_{y2})) \tag{7b}
 \end{aligned}$$

for  $m_{x1} = 1, \dots, 2N_{x1}$ ,  $m_{y1} = 1, \dots, N_{y1}$  and  $m_{x2} = 1, \dots, N_{x2}$ ,  $m_{y2} = 1, \dots, N_{y2}$ . The double integrals of the Green's function constituting the elements of the system matrix cannot be analytically evaluated unless an approximation for the integration domain is made. In particular, each rectangular pixel to which the integrals in (7a) and (7b) are referred, will be replaced by a circular disk of equal area, namely of radius  $a/\sqrt{\pi}$ . The difference is insignificant due to the small value of  $a$ . The representative integral of (7a), (7b) is written, by adopting the alternative cylindrical version of Green's function  $G(\rho, \phi, P, \Phi)$ , as follows:

$$\begin{aligned}
 M(\chi, \psi, x, y) &= \int_{y-\frac{a}{2}}^{y+\frac{a}{2}} \int_{x-\frac{a}{2}}^{x+\frac{a}{2}} G(\chi, \psi, X, Y) dXdY \\
 &= \int_{-\alpha/2}^{\alpha/2} \int_{-\alpha/2}^{\alpha/2} G(\chi, \psi, X+x, Y+y) dXdY \\
 &\cong \int_0^{2\pi} \int_0^{\alpha/\sqrt{\pi}} G(\mu(\chi, \psi, x, y), \gamma(\chi, \psi, x, y), P, \Phi) PdP d\Phi, \tag{8}
 \end{aligned}$$

where the functions of the line inclination passing through the points  $(\chi, \psi)$ ,  $(x, y)$  and the distance between them are defined below:

$$\gamma(\chi, \psi, x, y) = \arctan(\chi - x, \psi - y) \tag{9a}$$

$$\mu(\chi, \psi, x, y) = \sqrt{(\chi - x)^2 + (\psi - y)^2}. \tag{9b}$$

It is noted that  $\arctan(\alpha, \beta) \in [0, 2\pi)$ .

The analytical integrations are assisted by the following expansion of the Hankel function originating from the addition theorem [18, p. 363]:

$$\begin{aligned} & H_0^{(2)} \left( k_0 \sqrt{\mu^2 + P^2 - 2\mu P \cos(\gamma - \Phi)} \right) \\ &= \sum_{u=-\infty}^{+\infty} J_u(k_0 \min(\mu, P)) H_u^{(2)}(k_0 \max(\mu, P)) e^{ju(\gamma - \Phi)}, \end{aligned} \quad (10)$$

where  $J_u$  is the Hankel function of  $u$ -th order. In our approach  $\mu$  denotes the distance between the centers of two different pixels and therefore  $\mu > a/\sqrt{\pi} \geq P$ . If one takes into account common integrals of Bessel functions [18, p. 480] and (10), one obtains the formula below:

$$\begin{aligned} & \int_0^{2\pi} \int_0^{a/\sqrt{\pi}} H_0^{(2)} \left( k_0 \sqrt{\mu^2 + P^2 - 2\mu P \cos(\gamma - \Phi)} \right) P dP d\Phi \\ &= \frac{2a\sqrt{\pi}}{k_0} J_1 \left( k_0 \frac{a}{\sqrt{\pi}} \right) H_0^{(2)}(k_0\mu). \end{aligned} \quad (11)$$

In case  $\mu = 0$ , the relation is not functional and a special treatment should be applied instead:

$$\int_0^{2\pi} \int_0^{a/\sqrt{\pi}} H_0^{(2)}(k_0 P) P dP d\Phi = \frac{2}{k_0^2} \left[ k_0 a \sqrt{\pi} H_1^{(2)} \left( k_0 \frac{a}{\sqrt{\pi}} \right) - 2j \right]. \quad (12)$$

By combining (1), (8) and (11), (12) the following closed form expression is derived:

$$\begin{aligned} M(\chi, \psi, x, y) &\cong \frac{ja\sqrt{\pi}}{2k_0} J_1 \left( k_0 \frac{a}{\sqrt{\pi}} \right) H_0^{(2)}(k_0\mu(\chi, \psi, x, -y)) \\ &- \begin{cases} \frac{ja\sqrt{\pi}}{2k_0} J_1 \left( k_0 \frac{a}{\sqrt{\pi}} \right) H_0^{(2)}(k_0\mu(\chi, \psi, x, y)), & \chi \neq x \text{ or } \psi \neq y \\ \frac{j}{2k_0^2} \left[ k_0 a \sqrt{\pi} H_1^{(2)} \left( k_0 \frac{a}{\sqrt{\pi}} \right) - 2j \right], & \chi = x \text{ and } \psi = y. \end{cases} \end{aligned} \quad (13)$$

As a result, the  $(2N_{x1}N_{y1} + N_{x2}N_{y2}) \times (2N_{x1}N_{y1} + N_{x2}N_{y2})$  linear system (7a), (7b) takes the form:

$$\begin{bmatrix} (k_1^2 - k_0^2) \mathbf{M}_{11} - \mathbf{U}_{2N_{x1}N_{y1}} & (k_2^2 - k_0^2) \mathbf{M}_{12} \\ (k_1^2 - k_0^2) \mathbf{M}_{21} & (k_2^2 - k_0^2) \mathbf{M}_{22} - \mathbf{U}_{N_{x2}N_{y2}} \end{bmatrix} \cdot \begin{bmatrix} \mathbf{e}_1 \\ \mathbf{e}_2 \end{bmatrix} = - \begin{bmatrix} \mathbf{e}_{1,inc} \\ \mathbf{e}_{2,inc} \end{bmatrix}, \quad (14)$$

where  $\mathbf{U}_r$  is the  $r \times r$  unitary matrix. The vectors of the unknown quantities are given below:

$$\mathbf{e}_1 = [ E_1(x_1(1), y_1(1)) \quad \dots \quad E_1(x_1(2N_{x1}), y_1(N_{y1})) ]^T \quad (15a)$$

$$\mathbf{e}_2 = [ E_2(x_2(1), y_2(1)) \quad \dots \quad E_2(x_2(N_{x2}), y_2(N_{y2})) ]^T. \quad (15b)$$

The constant vectors of the incident quantities are given by:

$$\mathbf{e}_{1,inc} = [ E_{0,inc}(x_1(1), y_1(1)) \quad \dots \quad E_{0,inc}(x_1(2N_{x1}), y_1(N_{y1})) ]^T \quad (15c)$$

$$\mathbf{e}_{2,inc} = [ E_{0,inc}(x_2(1), y_2(1)) \quad \dots \quad E_{0,inc}(x_2(N_{x2}), y_2(N_{y2})) ]^T. \quad (15d)$$

It should be noted that in the above sequence of vector elements, the increment of the  $x$ -related index  $n/m_{x1/2}$  has priority over the  $y$ -related index  $n/m_{y1/2}$ . The same quoting rule is applied for the matrices below:

$$\mathbf{M}_{11} = \begin{bmatrix} M(x_1(1), y_1(1), x_1(1), y_1(1)) & \dots & M(x_1(1), y_1(1), x_1(2N_{x1}), y_1(N_{y1})) \\ \vdots & \ddots & \vdots \\ M(x_1(2N_{x1}), y_1(N_{y1}), x_1(1), y_1(1)) & \dots & M(x_1(2N_{x1}), y_1(N_{y1}), x_1(2N_{x1}), y_1(N_{y1})) \end{bmatrix} \quad (16a)$$

$$\mathbf{M}_{12} = \begin{bmatrix} M(x_1(1), y_1(1), x_2(1), y_2(1)) & \dots & M(x_1(1), y_1(1), x_2(N_{x2}), y_2(N_{y2})) \\ \vdots & \ddots & \vdots \\ M(x_1(2N_{x1}), y_1(N_{y1}), x_2(1), y_2(1)) & \dots & M(x_1(2N_{x1}), y_1(N_{y1}), x_2(N_{x2}), y_2(N_{y2})) \end{bmatrix} \quad (16b)$$

$$\mathbf{M}_{21} = \begin{bmatrix} M(x_2(1), y_2(1), x_1(1), y_1(1)) & \dots & M(x_2(1), y_2(1), x_1(2N_{x1}), y_1(N_{y1})) \\ \vdots & \ddots & \vdots \\ M(x_2(N_{x2}), y_2(N_{y2}), x_1(1), y_1(1)) & \dots & M(x_2(N_{x2}), y_2(N_{y2}), x_1(2N_{x1}), y_1(N_{y1})) \end{bmatrix} \quad (16c)$$

$$\mathbf{M}_{22} = \begin{bmatrix} M(x_2(1), y_2(1), x_2(1), y_2(1)) & \dots & M(x_2(1), y_2(1), x_2(N_{x2}), y_2(N_{y2})) \\ \vdots & \ddots & \vdots \\ M(x_2(N_{x2}), y_2(N_{y2}), x_2(1), y_2(1)) & \dots & M(x_2(N_{x2}), y_2(N_{y2}), x_2(N_{x2}), y_2(N_{y2})) \end{bmatrix}. \quad (16d)$$

#### 4. NUMERICAL RESULTS AND DISCUSSION

A set of computer programs has been developed to evaluate the electric field by solving the linear system (14) and by using (3). We are mainly

interested in measuring two field quantities whose variation is shown in the graphs of this section. The first quantity is the average field on the surface of the main island indicating the magnitude of the received signal across the larger region, namely, how well the area is covered in terms of wireless communication. Due to the tiny size of the second island we prefer to observe the maximum electric field on its surface, which is the second measured quantity and indicates if a single antenna is sufficient for the signal coverage of two neighboring supersea volumes.

Because of the large number of input parameters, some of them should be kept fixed throughout the numerical simulations (like the unitary excitation current  $I = 1$  A). The real permittivities of the scatterers materials are taken close to those possessed by several natural claddings, such as sand and vegetation:  $\text{Re}[\varepsilon_1] = \text{Re}[\varepsilon_2] = 10$  [19, 20]. Also, the characteristics of the second island (dimensions, material) are kept constant,  $L_2 = 200$  m,  $h_2 = 10$  m,  $\sigma_2 = 0.5$  S/m, as they do not significantly affect the calculated quantities.

The operating frequency is chosen low,  $1 \text{ kHz} < f < 20 \text{ kHz}$  with a typical value  $f = 10 \text{ kHz}$ , so that the rectangular scatterers are not electrically large. The dimensions of the first island can vary within the intervals  $1000 \text{ m} < L_1 < 2000 \text{ m}$  and  $5 \text{ m} < h_1 < 15 \text{ m}$  with average values  $L_1 = 1500$  m and  $h_1 = 10$  m. The inter-island distance satisfies the double inequality  $5 \text{ m} < D < 500 \text{ m}$  and usually equals  $D = 250$  m, while the height of the source belongs to the set  $15 \text{ m} < S < 45 \text{ m}$  with an average value  $S = 30$  m. The conductivity of the first island can change from zero to a substantial magnitude  $0 < \sigma_1 < 1$  S/m but is typically kept constant  $\sigma_1 = 0.5$  S/m. The dimension of each square pixel is taken on the order of  $a \cong |0.2/\sqrt{\varepsilon}|$  ( $\varepsilon$  denotes the respective complex relative permittivity) according to Richmond's rule of thumb [9]. As a result, the waveforms are converging and the results obtained are reliable.

In Fig. 2(a) we present the variation of the average electric field on the first island with respect to the length  $L_1$  for various heights  $h_1$ . It is observed that for increasing length the received signal is reduced, which makes sense since we use the same source for covering a larger area. Also, the curve for  $h_1 = 15$  m possesses the most substantial magnitudes as the dipole is not distant from the island's surface. In Fig. 2(b) the maximum field on the second volume is represented with respect to the same variables and parameters. The decaying behavior of the quantity with respect to  $L_1$  is again natural as the investigated region gets farther from the excitation source. Furthermore, the effect of the dipole is reduced for large  $h_1$  due to the opposite image developed (the rectangular volume is conducting). The same happens for low  $h_1$  as the first scatterer does not significantly support the primary

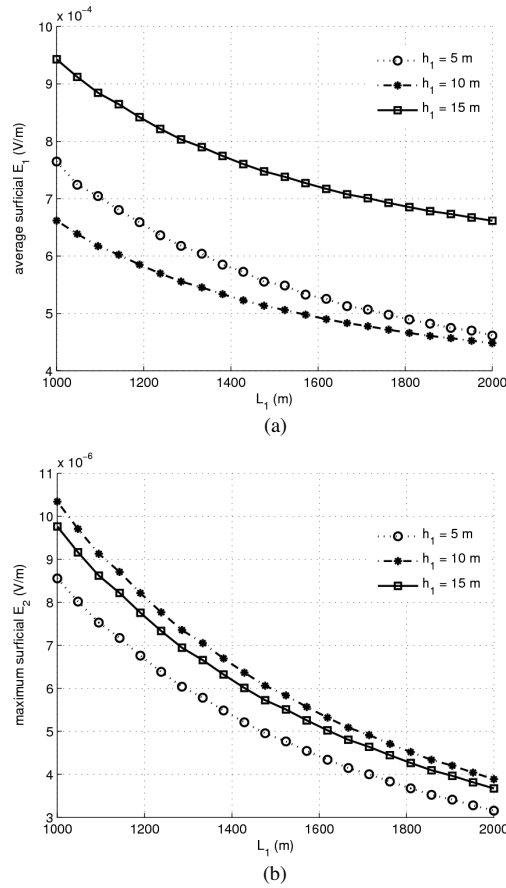


**Figure 2.** (a) The average electric field on the surface of the first island. (b) The maximum electric field on the surface of the second island, as function of the length of the first island for various first island heights. Plot parameters:  $\text{Re}[\varepsilon_1] = \text{Re}[\varepsilon_2] = 10$ ,  $\sigma_2 = 0.5 \text{ S/m}$ ,  $L_2 = 200 \text{ m}$ ,  $h_2 = 10 \text{ m}$ ,  $I = 1 \text{ A}$ ,  $D = 250 \text{ m}$ ,  $f = 10 \text{ kHz}$ ,  $S = 30 \text{ m}$ ,  $\sigma_1 = 0.5 \text{ S/m}$ .

radiation because of its small size. That is why the curve for  $h_1 = 10 \text{ m}$  shows the most significant values.

In Fig. 3(a) we present the variation of the average  $|E_1(x, h_1)|$  as function of the source height  $S$  for several conductivities  $\sigma_1$  of the first island. As the operating frequency is low, the imaginary parts of the complex permittivity are very large for  $\sigma_1 = 0.5, 1 \text{ S/m}$  and therefore the corresponding curves almost coincide with each other.

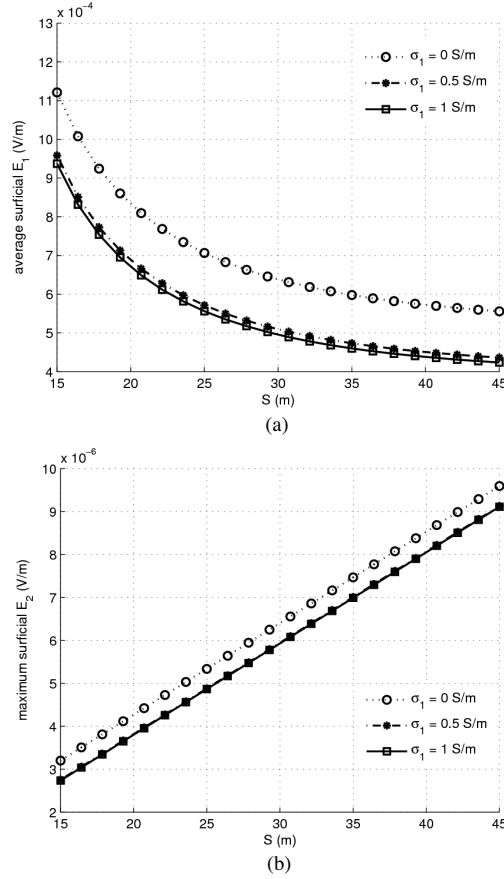


**Figure 3.** (a) The average electric field on the surface of the first island. (b) The maximum electric field on the surface of the second island as function of the source position for various conductivities of the first material. Plot parameters:  $\text{Re}[\epsilon_1] = \text{Re}[\epsilon_2] = 10$ ,  $\sigma_2 = 0.5$  S/m,  $L_2 = 200$  m,  $h_2 = 10$  m,  $I = 1$  A,  $D = 250$  m,  $f = 10$  kHz,  $L_1 = 1500$  m,  $h_1 = 10$  m.

Also, the values of the surface electric field are reduced for increasing  $S$  and  $\sigma_1$ , namely, the excitation force gets diminished because of the substantial distance and the powerful image, respectively. In Fig. 3(b) the curves representing the maximum signal on the second island are slope linearly upward with respect to  $S$ . The negative influence of the opposite image created internally to the first rectangular volume is decreased when the antenna is located higher. Again the curves

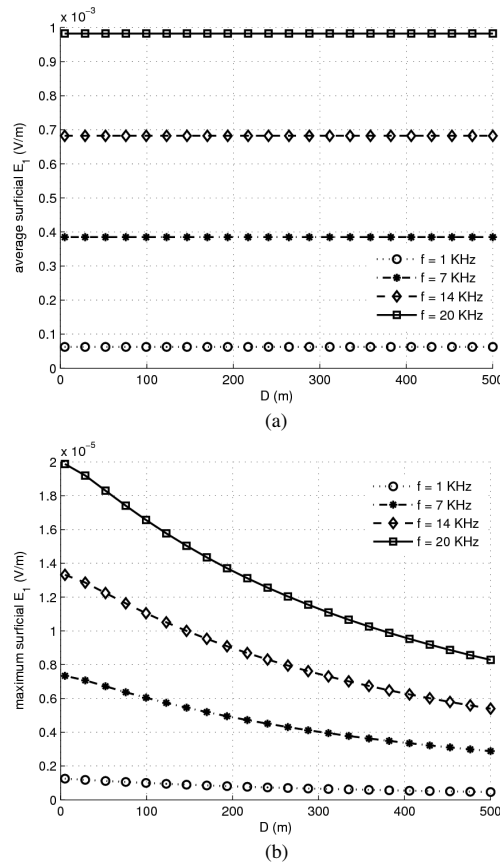


**Figure 4.** (a) The average electric field on the surface of the first island. (b) The maximum electric field on the surface of the second island, as function of inter-island distance for various operating frequencies. Plot parameters:  $\text{Re}[\epsilon_1] = \text{Re}[\epsilon_2] = 10$ ,  $\sigma_2 = 0.5 \text{ S/m}$ ,  $L_2 = 200 \text{ m}$ ,  $h_2 = 10 \text{ m}$ ,  $I = 1 \text{ A}$ ,  $S = 30 \text{ m}$ ,  $\sigma_1 = 0.5 \text{ S/m}$ ,  $L_1 = 1500 \text{ m}$ ,  $h_1 = 10 \text{ m}$ .

for  $\sigma_1 = 0.5, 1 \text{ S/m}$  concur and when the conductivity is zero, more significant magnitudes are recorded. It is also noteworthy that the field values in Fig. 3(b) are much smaller than those of the curves in Fig. 3(a). A similar observation can be made for Fig. 2 and it is attributed to the fact that the antenna is located above the first island for benefit of its own region; only in a supplementary sense can the source cover the second one.

In Fig. 4(a) we depict the average field on the main island

as function of the inter-island distance  $D$  for various operating frequencies  $f$ . It should be noted that the computed quantity is almost independent of the distance between the two supersea volumes. Such a conclusion could be anticipated as the presence of the second island has a rather insignificant influence on the first one. Moreover, for decreasing frequency (within a certain range), the field is reduced, probably because the electrical size and implicitly the reinforcing effect of the scatterer has been decreased. In Fig. 4(b) we present the maximum value of  $|E_2(x, h_2)|$  with respect to the same variables and parameters. With increasing  $D$  the signal decays as the observer on the second island is removed from the main structure. Finally, for lower frequencies the fall is less rapid as the electrical distance from the excitation source is diminished.

## 5. CONCLUSIONS

In this work, a model of the signal coverage of two neighboring islands is analyzed. A single source is located above the main island and the scattering of the produced waves by the perfectly conducting sea surface and the two rectangular volumes is studied. The scattering integral is manipulated by dividing the two dielectric scatterers into a large number of tiny square pixels and by assuming a constant field on each of these pixels. In this way, the total field on the island surfaces is approximately determined and observations about its dependencies are made.

The same technique can be applied to treat the case of non rectangular island shapes or inhomogeneous materials. Also, the metallic sea surface could be replaced by an imperfectly conducting half space in order to examine the electromagnetic penetration depth. Another interesting case could be the maximization of the received signal on both islands with respect to the position of the source for fixed material parameters. The extracted results can prove useful in real-world applications.

## REFERENCES

1. Umashankar, K. and A. Taflove, "A novel method to analyze electromagnetic scattering of complex objects," *IEEE Transactions on Electromagnetic Compatibility*, Vol. 24, No. 4, 397–405, November 1992.
2. Yang, C.-F. and T.-S. Wang, "A moment method solution for TM, and TE, waves illuminating two-dimensional objects above a lossy

- half space,” *IEEE Transactions on Electromagnetic Compatibility*, Vol. 38, No. 3, 433–440, August 1996.
3. Wait, J. R., “Electromagnetic fields of a vertical electric dipole over a laterally anisotropic surface,” *IEEE Transactions on Electromagnetic Compatibility*, Vol. 38, No. 10, 1719–1723, October 1990.
  4. Hu, J. and Z. Nie, “Improved electric field integral equation (IEFIE) for analysis of scattering from 3-D conducting structures,” *IEEE Transactions on Electromagnetic Compatibility*, Vol. 49, No. 3, 644–648, August 2007.
  5. Schlessinger, L., “Currents induced by a plane wave on an infinite wire above a flat earth,” *IEEE Transactions on Electromagnetic Compatibility*, Vol. 17, No. 3, 156–158, August 1975.
  6. Raemer, H. R. and D. D. Preis, “Aspects of parallel-polarized and cross-polarized radar returns from a rough sea surface,” *IEEE Transactions on Electromagnetic Compatibility*, Vol. 22, No. 1, 29–44, February 1980.
  7. King, R. W. P. and C. W. Harrison, “Electromagnetic ground-wave field of vertical antennas for communication at 1 to 30 MHz,” *IEEE Transactions on Electromagnetic Compatibility*, Vol. 40, No. 4, 337–342, November 1998.
  8. Wait, J. R., “Low frequency electromagnetic scattering from an island,” *IEEE Transactions on Antennas and Propagation*, Vol. 40, No. 4, 439–442, April 1992.
  9. Richmond, J. H., “Scattering by a dielectric cylinder of arbitrary cross section shape,” *IEEE Transactions on Antennas and Propagation*, Vol. 13, No. 3, 334–341, May 1965.
  10. Collin, R. E., *Field Theory of Guided Waves*, IEEE Press, New York, 1990.
  11. Valagiannopoulos, C. A., “Closed-form solution to the scattering of a skew strip field by metallic pin in a slab,” *Progress In Electromagnetics Research*, PIER 79, 1–21, 2008.
  12. Valagiannopoulos C. A., “Effect of cylindrical scatterer with arbitrary curvature on the features of a metamaterial slab antenna,” *Progress In Electromagnetics Research*, PIER 71, 59–83, 2007.
  13. Valagiannopoulos, C. A., “Single-series solution to the radiation of loop antenna in the presence of a conducting sphere,” *Progress In Electromagnetics Research*, PIER 73, 297–325, 2007.
  14. Valagiannopoulos, C. A., “Study of an electrically anisotropic cylinder excited magnetically by a straight strip line,” *Progress*

- In Electromagnetics Research*, PIER 73, 137–152, 2007.
15. Fikioris, G. and C. A. Valagiannopoulos, “Input admittances arising from explicit solutions to integral equations for infinite-length dipole antennas,” *Progress In Electromagnetics Research*, PIER 55, 285–306, 2005.
  16. Valagiannopoulos, C. A., “Arbitrary currents on circular cylinder with inhomogeneous cladding and RCS optimization,” *Journal of Electromagnetic Waves and Applications*, Vol. 21, No. 5, 665–680, 2007.
  17. Valagiannopoulos, C. A., “Electromagnetic scattering from two eccentric metamaterial cylinders with frequency-dependent permittivities differing slightly each other,” *Progress In Electromagnetics Research B*, Vol. 3, 23–34, 2008.
  18. Abramowitz, M. and I. A. Stegun, *Handbook of Mathematical Functions*, National Bureau of Standards, Washington D.C., 1964.
  19. Li, C., P. Tercier, and R. Knight, “Effect of sorbed oil on the dielectric properties of sand and clay,” *Water Resources Research*, Vol. 37, No. 6, 1783–1793, June 2001.
  20. Shrestha, B. L., H. C. Wood, and S. Sokhansanj, “Modelling of vegetation permittivity at microwave frequencies,” *IEEE Transactions on Geoscience and Remote Sensing*, Vol. 45, No. 2, 342–348, February 2007.